HHS Public Access

Author manuscript

J Immunol. Author manuscript; available in PMC 2016 May 15.

Published in final edited form as:

J Immunol. 2015 May 15; 194(10): 4784–4795. doi:10.4049/jimmunol.1403158.

Young, proliferative thymic epithelial cells engraft and function in aging thymuses

Mi-Jeong Kim[*,†], **Christine M. Miller**[*,†,‡], **Jennifer L. Shadrach**[*,†,‡], **Amy J. Wagers**[*,†,‡], and **Thomas Serwold**[*,†,§]

[*]Joslin Diabetes Center, Boston, MA 02215, USA

[†]Harvard Stem Cell Institute, Cambridge, MA 02138, USA

[‡]Howard Hughes Medical Institute and Department of Stem Cell and Regenerative Biology, Paul F. Glenn Laboratories for the Biological Mechanisms of Aging, Harvard Medical School, Harvard University, Cambridge, MA 02138, USA

Abstract

The thymus reaches its maximum size early in life and then begins to shrink, producing fewer T cells with increasing age. This thymic decline is thought to contribute to age-related T cell lymphopenias and hinder T cell recovery following bone marrow transplantation. While several cellular and molecular processes have been implicated in age-related thymic involution, their relative contributions are not known. Using heterochronic parabiosis, we observe that young circulating factors are not sufficient to drive regeneration of the aged thymus. In contrast, we find that resupplying young, engraftable thymic epithelial cells to a middle-aged or defective thymus leads to thymic growth and increased T cell production. Intrathymic transplantation and *in vitro* colony forming assays reveal that the engraftment and proliferative capacities of thymic epithelial cells diminish early in life, whereas the receptivity of the thymus to thymic epithelial cell engraftment remains relatively constant with age. These results support a model in which thymic growth and subsequent involution are driven by cell intrinsic changes in the proliferative capacity of thymic epithelial cells, and further show that young thymic epithelial cells can engraft and directly drive the growth of involuted thymuses.

Introduction

The age-related decrease in the size of the thymus, known as thymic involution, is an evolutionarily conserved property of the adaptive immune system, documented in fish, birds, and mammals (1). In humans, thymic involution begins around the time of birth and continues throughout life (2). In mice, the thymus reaches its maximum size at 3–4 weeks of age, and then begins to involute (3, 4). Changes in circulating factors, hematopoietic

[§]Corresponding author: Thomas Serwold, One Joslin Place, Joslin Diabetes Center, Boston, MA 02215., thomas.serwold@joslin.harvard.edu., Phone: 617-309-2530., FAX: 617-309-4218.

Disclosures

The authors have no financial conflicts of interest.

progenitor cell number and function, thymic epithelial cells (TECs) and the thymic microenvironment have all been implicated in age-related thymic decline (5).

Circulating factors were implicated in thymic involution by experiments involving castration of aged male rodents; after castration, thymuses underwent a striking regeneration that could be inhibited by administration of testosterone (6–8). In addition to testosterone, the glucocorticoid hormone cortisol also has deleterious effects on the thymus (9, 10). Circulating factors, including insulin-like growth factor-1 (IGF-1), interleukin-7 (IL-7), IL-22, and keratinocyte growth factor (KGF) can also enhance thymus growth and/or regeneration (11–14). Thus, circulating factors can have profound positive, as well as negative, effects on thymus size. However, direct roles for circulating factors in normal thymic involution have not yet been identified.

Age-related thymic shrinkage may also result from an insufficient number or quality of T cell progenitors. Early thymic progenitors (ETPs), a rare population of cells within the thymus that give rise to all subsets of developing T cells, decline in number and function with age (5, 15, 16). ETPs develop directly from thymus seeding cells, which home to the thymus from the bone marrow (17, 18). The diminished number of ETPs in the aged thymus may result from age-related decreases in the T lineage differentiation potential of bone marrow progenitors and hematopoietic stem cells (HSCs); however, the observed decrease in lymphoid potential of HSCs occurs later in life than the initiation of thymic involution. Nevertheless, loss of lymphoid progenitors may play an important role in thymic involution, especially late in life.

Non-circulating, thymus intrinsic factors also strongly influence thymus size. Fetal thymuses implanted under the kidney capsules of young or aged mice grow equally well, indicating that circulating factors in aged mice are not acutely toxic to young thymocytes, and suggesting that early thymic growth is driven by thymus intrinsic factors (19, 20). However, these studies were performed using transplanted fetal thymuses, which are programmed to undergo several weeks of rapid growth, and therefore it remained possible that circulating factors may play a major role in controlling the size of mature thymus.

Adipocytes increasingly populate the aged thymus, and have been implicated in diminished thymic function (2, 21). In thymuses that undergo accelerated adipogenesis because of loss of the ghrelin signaling pathway, there is accelerated involution, suggesting that replacement of the normal thymic stroma with adipocytes may drive thymus shrinkage and loss of T cell production, perhaps through the elaboration of cytotoxic inflammatory mediators (22). In agreement with this model, thymuses of mice that lack the NLRP3 inflammasome, which is activated in response to adipocyte-derived inflammatory lipids, involute more slowly and undergo accelerated thymic regeneration after irradiation (23). These studies suggested, but did not directly show, that the thymic microenvironment becomes progressively more toxic with age, and that gradual accumulation of adipocytes may be at least partially responsible for age-related thymic decline.

Loss of function of TECs with age has been specifically implicated in thymic involution (24, 25). TECs play multiple essential roles in driving T cell development; they express Stem

Cell Factor (SCF; c-Kit ligand), IL-7, Delta like 4 (Dll4), and high levels of Major Histocompatibility Complex class I (MHCI) and class II molecules (MHCII), all of which are essential for normal T cell development (26–29). TECs also express several different chemokines that recruit T cell progenitors from the blood and direct their migration within the thymus (30). Several lines of evidence suggest that the proliferation and function of TECs dictates thymus size. The most striking evidence of the importance of TECs in determining thymus size is the phenotypes of mice in which TECs are aberrantly proliferative. Murine TECs that transgenically overexpress the cell cycle protein, Cyclin D1, as well as TECs that are deficient in the Retinoblastoma cell cycle regulator family of proteins, are hyperproliferative (31, 32). The thymuses of these genetically modified mice are functionally and architecturally normal but grow continuously and eventually cause death by asphyxiation. From these studies, it is clear that regulation of TEC proliferation is critical for maintaining normal thymus size.

Expression of the transcription factor Foxn1 is required for TEC differentiation, and mice lacking Foxn1 completely lack thymuses (33). Experiments using blastocyst chimeric mice containing mixtures of wild type (WT) and Foxn1-deficient ES-cells found that thymus size was dependent upon the absolute number of functional thymic epithelial progenitors within the embryo (34). Foxn1 itself appears to be downregulated in TECs with age, and restoration of Foxn1 expression within the aging thymus can drive thymus regeneration (35, 36). This observation suggested that loss of TEC function with age plays an important role in thymic involution, however, it was unclear whether the loss of TEC function resulted from acute environmental signals that drove changes in TEC function, or whether TECs underwent programmed, intrinsic changes that led to their dysfunction.

In this study, we sought to determine the relative importance of systemic, circulating, and thymus intrinsic factors in determining thymus size during aging, and we further sought to directly test whether the involuted thymus could be induced to grow by transplanted, functional TECs. We used heterochronic parabiosis to assess whether age-related changes in circulating factors or hematopoietic cells impact endogenous thymus size. We also used intrathymic transplantation and *in vitro* colony forming assays to evaluate age-related changes in TEC proliferative and engraftment capacity, as well as age-related changes in the thymic microenvironment. These experiments establish the utility of intrathymic transplantation of TECs as a means of evaluating the thymic microenvironment, characterizing TEC developmental potential, and as a means of modulating T cell development. Intrathymic transplantation of TECs reveals that the involuted and young intrathymic environments are equally receptive to TECs, and also reveals that TECs incur cell intrinsic reductions in engraftability potential with age; moreover, resupplying young, engraftable TECs to involuted thymuses of middle-aged mice leads to renewed thymic growth and T cell production.

Materials and methods

Animals

All the mice used in the current study were derived from the C57BL/6 background. Retired breeder female mice (middle-aged) were purchased from Taconic. GFP-transgenic mice

contained a GFP transgene under the control of the β-actin promoter (37). Red Fluorescent Protein (RFP)-transgenic mice contained a CAG promoter driving RFP inserted into the Rosa locus (38). Aged mice for parabiosis experiments (21–23 months) were obtained from the National Institute of Aging. Young CD45.1 and CD45.2 C57BL/6 mice, as well as MHCII$^{-/-}$ mice were obtained from the Jackson Laboratory. All mice were housed in the Joslin Diabetes Center animal facility. The Joslin Institutional Animal Care and Use Committee approved all experimental protocols involving mice.

Parabiosis

Parabiosis was performed as previously described (39, 40). Sex matched C57BL6 mice were used for parabiosis. Young C57BL/6 (2 months) or aged C57BL/6 mice (21–23 months) were parabiosed to young C57BL/6.SJL mice (2 months, CD45.1) to enable detection of donor hematopoietic chimerism. For isochronic old pairs, CD45 distinction was not possible, since aged CD45.1 mice were not available.

Thymic epithelial cell isolation

The thymus was removed from the thoracic cavity and put into DMEM/F12 (Life Technologies) medium, where it was minced into small pieces using a scalpel, followed by rocking for 3 minutes. The released thymocytes were removed, and fresh DMEM/F12 was added to the remaining thymic tissue fragments. Tissue fragments were incubated with collagenase & dispase (5 mg/ml) (Roche Diagnostics) or collagenase IV (0.25 mg/ml) & papain (0.25 mg/ml) (Worthington Biochemical Corporation) and DNase I (0.1 mg/ml) (Roche Diagnostics) for 30 min at 37°C. Digested tissue samples were pipetted up and down using a wide-bore pipet tip and filtered through 70 μm nylon mesh to remove any undigested fragments of tissue. Dispersed cells were washed with PBS containing 2% bovine calf serum (HyClone).

Flow cytometry

TECs were stained with antibodies to CD45, epithelial cell adhesion molecule (EpCAM), Ly-51, *Ulex Europaeus* Agglutinin I (UEA), MHCII, and CD80. In some experiments, as noted in the text, single thymic cells in suspension were stained with APC/Cy7 anti-mouse EpCAM (Biolegend) and anti-Cy7 MicroBeads (Miltenyi), and EpCAM^{+} TECs were positively selected by using a magnetic column (Miltenyi). For analysis of thymocytes and splenocytes, tissues were dispersed by grinding between frosted slides and red blood cells were removed by lysis in ACK solution (150 mM NH_4Cl, 10 mM $KHCO_3$, 0.1 mM EDTA). Antibodies for all stains are listed in Supplemental Table 1. Stained cells were analyzed on either an LSRII flow cytometer (BD Biosciences) or sorted on a FACSAria cell sorter (BD Biosciences). The flow cytometry data were analyzed using FlowJo (Treestar Inc.)

Intrathymic transplantation

Total dispersed thymic cells or EpCAM-positive or negative cells from fetal or postnatal mice were prepared as described in the ‘*Thymic epithelial cell isolation’* and ‘*Flow cytometry’* sections above. Cells were kept on ice until mice were ready for the injection. Intrathymic injections were performed as previously described (41). Mice were anesthetized

by intraperitoneal injection of 250 mg/kg body weight of 2,2,2-tribromoethanol (Avertin, Sigma) in saline. The unconscious mice were then placed in supine position, and a small incision was made by cutting 0.5 cm of the skin and manubrium to expose thymus within the thoracic cavity. Five to 10 μl of cells in suspension were drawn into a Hamilton syringe equipped with a 30 Gauge needle (Fisher Scientific), and then injected into one thymic lobe. One or two wound clips (Fisher Scientific) were applied to close the incision. The surgery survival rate was greater than 99%. The recipient thymuses with donor GFP^+ or RFP^+ cells were recovered from mice at the specified time points (e.g. 1-month post-intrathymic transplantation), and each thymus was examined for the presence of donor GFP^+ or RFP^+ cells, using an Olympus IX51 inverted fluorescence microscope (Olympus) attached with DP72 camera with cellSens software (Olympus).

In vitro culture of TECs

Sorted GFP^+ TECs were plated onto irradiated murine embryonic fibroblasts (MEFs) (60 Gray) and cultured in MCDB153 medium (Sigma) supplemented with 10% fetal bovine serum (HyClone), 50 units/ml penicillin and 50 μg/ml streptomycin (Life Technologies), 2 mM L-glutamine (Life Technologies) and 1 mM sodium pyruvate (Life Technologies), and 10 μM p160ROCK inhibitor, Y-27632 (TOCRIS Bioscience). TEC colonies were imaged using an inverted fluorescence microscope (Olympus), or by colony staining. For colony staining, cultured TECs were fixed in 4% paraformaldehyde (PFA) for 10 min, washed in PBS, and then stained with 1% Rhodamine B (Sigma) in PBS at 60°C for 10 min. Images were taken with a Stylus Verve 5.0 camera (Olympus).

Histology

Recipient thymuses that received GFP^+ or RFP^+ donor cells by intrathymic injection were removed and immediately fixed in 4% PFA at 4°C overnight. The fixed tissues were immersed in graded sucrose solutions and then embedded in OCT compound (Sakura). Frozen tissues were sectioned (5–10 μm) using a cryostat (Microm HM 550, Thermo Scientific). Sections were fixed in cold acetone, washed in PBS, and mounted in Fluoromount-G (SouthernBiotech) medium, and were examined to locate sections containing donor GFP^+ or RFP^+ cells. For some experiments, sections were stained with the lectin UEA, or with antibodies to Psmb11 or I-A/I-E (MHCII). Nuclei were visualized using DAPI (Sigma). Epifluorescence images were taken using an Axioplan 2 imaging microscope (Zeiss) equipped with a SPOT digital camera and software (SPOT Imaging), and confocal images were taken with a LSM 710 Duo (Zeiss) confocal microscope with an AxioCam camera (Zeiss). Serial images were compiled using the Z-stack function. Adobe Photoshop CS4 program was used to convert color images to gray scale. Tile and binary images were generated using BZ-X700 microscope (Keyence).

Results

Parabiosis of young and old mice does not cause regeneration of the aged thymus

To evaluate globally whether circulating factors and cells that change with age control thymus size, we analyzed the thymuses of young and old C57BL/6 mice that had been joined in heterochronic parabiosis, a surgical intervention that produces a shared circulation

between two animals. The parabiotic model has been used extensively to investigate the influence of blood-borne signals on aging phenotypes, and such studies have identified both cellular (42) and molecular mechanisms underlying the aging and rejuvenation of a variety of tissues (40, 43–46). Parabiotic mice begin sharing a circulatory system by 2–3 days after joining and achieve a steady state of ~50% chimerism for circulating hematopoietic cell lineages in 7–10 days. Thus, we reasoned that if an age-variant cell type or factor circulating in the blood contributes substantially to the age-related decline of thymus size, then animals joined in heterochronic parabiosis should show changes in thymus size when compared to isochronically joined (either young-young or aged-aged) control pairs. Mice were joined at 2 months of age (young) or 21–23 months of age (aged), and their thymuses were analyzed 1 month after joining. The young-isochronic and heterochronic pairs were congenic at their CD45 loci, enabling determination of the contribution of partner-derived thymus seeding cells using antibodies to CD45.1 and CD45.2. We could not generate CD45 congenic pairs of old-isochronic mice, due to the unavailability of aged CD45.1 animals; however, prior experience with this model indicates that old-isochronic animals develop peripheral chimerism at a rate that is indistinguishable from young-isochronic and heterochronic pairs (42).

The thymuses of all heterochronic and isochronic parabiotic mice became chimeric with their partner's cells, to varying degrees (Fig. 1A, Fig. 1B). Furthermore, partner-derived thymocytes contributed to each major thymocyte subset, including all the immature double negative subsets that are distinguished by c-kit and CD25 (DN1-DN4), as well as the $CD4^+CD8^+$ subset, and the more mature single positive subsets. These results are consistent with previous parabiotic experiments showing that blood-derived thymus seeding cells cross the parabiotic anastomoses and seed the partner's thymus, where they undergo apparently normal T-lineage differentiation (47). Isochronic young parabionts averaged 9–13% thymus chimerism (range 1–50%, Fig. 1B). In contrast, heterochronic parabionts showed significantly increased contribution of young CD45.1 cells to the aged thymuses, (average chimerism = 37%, range 6–72%) and a significantly decreased contribution of aged cells into the young thymuses (average chimerism = 3%, range 0–12%). These dramatic differences in thymocyte contribution between the heterochronic parabionts are unlikely to be attributable to the congenic CD45 alleles, as congenic pairs of young-isochronic parabionts showed equivalent cross-seeding, and instead suggest a significant competitive advantage of young thymus seeding cells and/or thymocytes in comparison to analogous populations of aged cells.

Despite the substantial engraftment of young thymocytes into the aged thymuses of heterochronic parabionts, the thymuses of the aged partners did not show an increase in total cellularity (Fig. 1C). In fact, the aged partners within the heterochronic pairs had significantly smaller thymuses than the aged-isochronic parabionts. These results indicate that the younger mice contain more efficient thymus seeding progenitors than old mice, but that the young circulatory system and progenitors are not, by themselves, capable of driving regeneration of the aged thymus. Furthermore, there was no correlation between donor chimerism and thymus cellularity; even the aged parabionts with the highest percentage of young thymocyte chimerism did not show increased thymic cellularity (Supplemental Figure 1). The failure of the young circulatory system to regenerate the aged thymus and the

inability of the aged circulatory system to shrink the young thymus suggest that the major determinants of thymus size in aged mice are not circulating, and instead are likely intrinsic to the thymus.

Thymic epithelial cells engraft and function after intrathymic injection

Thymus intrinsic components include stromal cells such as mesenchymal, epithelial, and endothelial cells, as well the extracellular matrix. To directly evaluate the role of thymus intrinsic components in age-related thymic decline, we established a new system for intrathymic injection of TECs, as well as other stromal cells. Intrathymic injection of hematopoietic progenitors is a well-established technique for studying the differentiation of T cell progenitors, but this method has not been widely applied to the study of thymic stromal components (48). To test whether intrathymically injected thymic stromal cells could engraft and function, we isolated fetal thymic cells from E15–17 embryos that ubiquitously expressed GFP under the β-actin promoter (37). The fetal thymuses were proteolytically dissociated into single cells and injected intrathymically into MHCII$^{-/-}$ mice, which fail to efficiently drive positive selection of CD4^{+} T cells and have both thymic and peripheral deficiencies of CD4^{+} T cells (49). Thirty days after intrathymic injection of wild type fetal thymic cells, positive selection of CD4^{+} T cells was partially restored in the thymuses of MHCII$^{-/-}$ mice (Fig. 2A, Fig. 2B). This recovery of CD4^{+} T cell selection was also reflected in the periphery, where the frequency of naïve CD4^{+} T cells increased significantly (Fig. 2C). The ability of intrathymically injected fetal thymic cells to rescue CD4^{+} T cell development in MHCII$^{-/-}$ mice suggested that wild type MHCII^{+} donor cells had engrafted in the recipient thymuses. Moreover, because MHCII-expressing TECs are the major drivers of T cell positive selection (26), these results suggested that donor TECs functionally engrafted in the recipient thymuses after intrathymic injection.

To visualize TEC engraftment after intrathymic injection of GFP^{+} thymic stromal cells into MHCII$^{-/-}$ mice, we analyzed the thymuses of recipient mice by immunofluorescence. Intrathymic injection of dissociated thymic cells from GFP-transgenic donors resulted in the engraftment of networks of donor-derived cells that strongly resembled TECs (Fig. 2D). In addition, injection of purified EpCAM^{+} cells from GFP-transgenic donors into MHCII$^{-/-}$ recipients resulted in a similar pattern of engrafted GFP^{+} donor cells, clearly indicating that purified EpCAM^{+} TECs can engraft and establish typical TEC networks after intrathymic injection (Fig. 2E). Furthermore, donor TECs maintained MHCII expression (Fig. 2E), consistent with their ability to rescue T cell development in MHCII$^{-/-}$ mice. Thus, after intrathymic transplantation, TECs form networks and maintain their ability to drive T cell development.

Intrathymically transplanted TECs proliferate within the recipient thymus

To understand TEC dynamics following transplantation, total dispersed thymic cells derived from postnatal day 1 (P1) GFP-transgenic mice were intrathymically injected into MHCII$^{-/-}$ mice (3-month old), and thymuses were analyzed at day 3 and day 30 by fluorescence. At day 3 after transplantation, donor TECs appeared as disorganized clusters of cells (Fig. 3A). In contrast, by 30 days post-transplantation, TECs were organized into large spherical clusters containing hundreds to thousands of highly interconnected cells that resembled the

architecture of normal TECs (Fig. 3A). This extensive, patterned engraftment of TECs after intrathymic transplantation indicated that transplanted TECs either proliferated or re-organized within the recipient thymus.

It was important to distinguish whether the organized structures formed by donor TECs resulted from proliferation or from delayed organization of the transplanted cells. The low yield of donor TEC recovery from recipient mice precluded BrdU incorporation assays. Therefore we performed an *in vivo* colony forming assay. In this assay, equal numbers of dispersed GFP^+ and RFP^+ TECs are mixed together and injected into the thymus of a recipient mouse. Proliferation of these non-migratory cells is predicted to lead to the formation of clonally derived cell colonies. These colonies would appear in tissue sections as large areas covered exclusively either by GFP^+ TECs or alternatively, by RFP^+ TECs (Fig. 3B; Proliferation). Alternatively, if transplanted TECs failed to proliferate, they would not form colonies, but would form networks with their randomly associating GFP^+ and RFP^+ neighboring cells. This outcome would appear in tissue sections as highly interspersed GFP^+ and RFP^+ TECs, with few or no large clusters of either color (Fig. 3B; Non-proliferation). Consistent with the former prediction, at day 30 post-transplantation, recipient thymuses contained primarily clusters of exclusively GFP^+ or exclusively RFP^+ TECs (Fig. 3C). These data indicate that intrathymically injected TECs engraft, proliferate and form canonical, functional TEC networks after intrathymic injection.

Transplantation of fetal thymic cells into involuted thymuses drives thymus growth and renewed T cell production

The finding that fetal thymic cell transplantation could rescue the defective immune function in $MHCII^{-/-}$ mice suggested the possibility that the transplantation of fetal TECs could rejuvenate involuted WT thymuses and subsequently restore robust T cell production. The parabiosis experiments were performed with 21–23 month old mice (Fig. 1); however, the fragile state of these mice precluded intrathymic injections. Therefore, to test the possibility of cell-mediated regeneration of the aged thymus, we utilized 9–12 month old, “middle-aged” recipient mice, which also have involuted thymuses (see Fig. 8F for comparison). Thymuses from GFP-transgenic E14.5 or E15.5 fetuses were proteolytically dispersed into single cells and intrathymically injected into middle-aged female mice. After 45 days, the thymuses of the recipient mice were removed and analyzed. Thymic lobes transplanted with fetal cells were significantly larger than the non-transplanted lobes, clearly indicating that the injected fetal thymic cells drove thymic growth (Fig. 4A). The GFP^+ donor cells engrafted over a large area of the recipient lobes, as revealed by GFP fluorescence of the whole lobes (Fig. 4B, Fig. 4C, Fig. 4D).

Histological sections revealed that the engrafted cells were primarily composed of TECs that were present in stereotypical TEC networks (Fig. 5A). Immunostaining revealed that the engrafted TECs expressed MHCII, and were composed of both Psmb11-expressing cTECs and UEA-expressing mTECs (Fig. 5A). To further confirm donor TEC engraftment, recipient thymuses were proteolytically dispersed and analyzed by flow cytometry, which revealed a distinct population of donor-derived, $CD45^-EpCAM^+GFP^+$ TECs (Fig. 5B). Staining of the TECs with antibodies to Ly-51 and CD80, as well as the lectin UEA, clearly

identified donor-derived cTECs, as well as immature and mature mTEC subsets. Thus, injection of dispersed fetal thymic cells into thymuses of middle-aged mice results in substantial engraftment of TECs and significant growth of engrafted thymic lobes.

The transplantation of fetal thymic cells into the thymuses of middle-aged mice also led to increased production of naïve T cells, as measured by the frequency of $CD62L^{+}CD4^{+}$ T cells in the spleens of recipient mice (Fig. 5C). However, the increase in splenic naïve T cell frequencies did not correlate with the levels of donor-cell engraftment in recipient mice (Supplemental Figure 2). There was also a trend toward increased naïve $CD8^{+}$ T cells in the transplanted mice. Overall, these data show that transplantation of fetal thymic cells into thymuses of middle-aged mice leads to substantial engraftment of donor TECs, induction of thymus growth, and increases in the production of naïve T cells from endogenous, aged T cell progenitors.

Multiple cell types are present in the young thymus, including TECs, other stromal cell populations, developing thymocytes, and other hematopoietic $CD45^{+}$ lineages. To distinguish whether engrafted TECs or alternatively, a non-TEC population drives thymic growth, we sorted and transplanted into thymuses of middle-aged mice either TECs ($CD45^{-}EpCAM^{+}$) or the remaining non-TECs ($CD45^{+}EpCAM^{-}$), including all cells of the hematopoietic, mesenchymal, and endothelial lineages. We found that thymuses that received TECs exhibited growth specifically in the transplanted lobes (Fig. 6A). Interestingly, thymuses that received non-TECs, while showing no lobe-specific regeneration, also trended larger than the control recipient thymuses (Fig. 6B). Given the large degree of variability in thymus sizes between mice in this study, it is possible that the trend toward larger thymuses in the recipients of non-TECs was the result of statistical noise. In contrast to the large variability in thymic size between mice, intra-mouse variability in thymic lobe size was remarkably small; thus the lobe-specific growth induced by transplanted TECs shows that these cells are uniquely potent at driving growth of involuted thymuses.

Thymus receptivity to TEC engraftment remains constant with age

With age, the thymus loses some of its characteristic organization and becomes increasingly populated with adipocytes. It has been hypothesized that the adipogenic thymic environment of the involuted thymus is hostile to thymic stromal cells and plays a role in thymic shrinkage with age (21). To test this hypothesis, we transplanted TECs from P1 GFP^{+} or RFP^{+} mice into recipient mice that ranged in age from 1 to 10 months. At one-month post-transplantation, thymuses were screened for TEC engraftment. Remarkably, donor-derived TECs were equally abundant in recipient thymuses from mice of all ages (Fig. 7A, Fig. 7B). Thus, the thymic microenvironments of both young and middle-aged mice are receptive to TEC transplantation and proliferation. This result is consistent with the finding that fetal TECs engraft and drive growth of the middle-aged thymus (Fig. 4, Fig. 5, Fig. 6). Moreover, together with the results from the heterochronic parabiosis (Fig. 1), these data indicate that the middle-aged thymus remains receptive to the proliferation and development of both thymocytes and TECs.

TEC engraftment potential diminishes rapidly with donor age

Since the thymic microenvironments of both young and middle-aged mice appeared to be equally receptive to TEC transplantation and proliferation, we next asked whether TECs undergo intrinsic proliferative changes with age that might account for the small size of the aged thymus. TECs isolated from the thymuses of mice ranging in age from 1-day to 4-months, were injected into two-month old recipient mice. At one-month post-transplantation, thymuses were harvested and donor TEC engraftment was evaluated. Thymuses transplanted with P1 TECs contained large networks of engrafted cells, whereas thymuses transplanted with TECs from 1, 2.5, or 4-month old mice contained only sparse donor cells and no network formation (Fig. 7C, Fig. 7D). These data clearly indicate that the *in vivo* engraftment and proliferation capacity of TECs declines rapidly with age.

The number of TEC colony forming cells decreases rapidly with age

The striking age-related decline in TEC engraftment potential could result from diminished proliferative potential of TECs with age. Phenotypically, TECs undergo dramatic changes over the course of life (24). In the embryo, and shortly after birth, Ly-51$^+$ cTECs predominate, whereas by 9 days after birth, UEA$^+$ mTECs predominate (Fig. 8A). To determine whether these age-related phenotypic changes correlate with changes in TEC proliferative capacity with age, we developed an *in vitro* colony forming assay that efficiently promoted the survival and growth of TECs. This assay utilized a base medium optimized for epithelial cells, as well an inhibitor of rho-associated kinase (p160ROCK inhibitor Y-27632). ROCK inhibitor has been previously shown to enhance the survival of embryonic stem cells during passaging and cell sorting (50). We found that inhibition of ROCK also enhanced the survival and proliferation of sorted primary TECs in culture (Fig. 8B).

Using this colony-forming assay, we measured the proliferation of TECs sorted from mice of different ages. During 5 days in culture, TECs of E14.5 as well as postnatal P4 mice rapidly proliferated to form large colonies (Fig. 8C, Fig. 8D, plating efficiency mean = 58% for E14.5, and 45% for P4). TECs from P9 gave rise to similar, large colonies, but at a slightly lower plating efficiency (mean = 31%). In contrast, TECs from 1-month and older mice were much less efficient at forming colonies in culture (plating efficiency = 2–13%), although the colonies that did arise were similar in size to the colonies derived from P4 and P9 mice. These results indicate that the frequency of highly proliferative TEC colony-forming cells declines rapidly in postnatal life (between P9 and P30), and indicate that an age-related loss of a subset of highly proliferative TECs, rather than a deficient proliferative potential of all TECs, likely underlies the rapid decrease in TEC engraftment potential with donor age seen in our *in vivo* studies (Fig. 7).

Interestingly, the colony forming frequency of the TEC population closely tracks with the frequency of cTECs within the TEC population (Fig. 8E), suggesting that the colony forming cells may derive from a subset of cells within the cTEC population. This finding is consistent with a recent study that identified a TEC progenitor within this population (51).

In both male and female mice, the thymus grows rapidly for the first 4 weeks of life, reaches a maximum, and then begins to shrink (Fig. 8F). Remarkably, the loss of TEC colony forming cells exactly matches this timeline, suggesting a role for the colony-forming TECs in early thymus growth.

Discussion

In this study, we systematically evaluated three possible contributors to the small size of the aged thymus: age-related changes in circulatory factors, changes within the thymic stromal environment, and changes in TEC proliferative potential. We find that engraftable, colony forming TECs are only abundant in the young, growing thymus and are rare in the thymuses of adult and aged mice. We also find that intrathymic transplantation of these young, engraftable TECs leads to substantial donor TEC engraftment, thymus growth, and increased T cell production.

Heterochronic parabiosis revealed that the thymuses of aged mice, when exposed to the circulating factors and cells of younger mice, became disproportionately colonized by young T cell progenitors. Conversely, aged circulating progenitors are either less abundant or less adept at colonizing the thymuses of young mice. Previous studies have observed that HSCs in aged mice have reduced lymphoid potential, especially in regards to B cell potential (52). The loss of T cell potential of aged HSC, while apparent in some studies (15, 53), has been less consistently observed (54). This inconsistent observation of T cell deficiencies in aged progenitors has been attributed to the use of irradiation in transplantation studies (15). Our results may help to explain some of the inconsistencies in measurements of T cell potential of aged HSC. In the heterochronic parabionts, there was clearly a loss of T lineage potential within the aged hematopoietic system. However, once the thymus seeding cells from aged mice arrived at the thymuses of young mice, they proliferated and differentiated proportionately to their younger counterparts, suggesting that aged thymocytes are as capable as young thymocytes to proceed through the basic steps of T cell development.

Surprisingly, while the thymuses of aged mice became heavily colonized by younger thymocytes in heterochronic parabionts, the aged thymuses did not grow larger, indicating that young thymus seeding cells are not sufficient to drive re-growth of the aged thymus. This finding is consistent with a previous study that noted a failure of heterochronic parabiosis to induce aged thymic growth (55). Our parabiosis data also suggested that the circulatory system of 2-month old mice might contain factors that actually promote thymic involution. In this regard, it is worth noting that the thymuses of 2-month old mice, while larger than those of 18-month old mice, are undergoing more rapid involution; our data indicate that this rapid involution may be partly driven by circulating factors. However, in the absence of the identification of involution-driving factors in young mice, multiple possible interpretations of this observation exist. For example, we have not ruled out the possibility that stress levels may be higher in the heterochronic parabionts, and that the old thymuses might be more sensitive to stress-mediated thymus toxicity. The observation of thymus-inhibitory factors in the 2-month old circulatory system also reveals a limitation to the parabiosis model in the study of thymic growth factors. The murine thymus reaches maximal size over the course of the first 4 weeks of life, and involutes thereafter. Given that

parabiosis requires mice of roughly similar size and feeding abilities, all heterochronic parabiosis experiments between mice are necessarily done in mice with involuting thymuses. Therefore, it remains unexplored whether circulatory factors drive thymus growth in mice younger than 4 weeks. Nevertheless, the parabiosis experiments performed in this study suggest that circulatory factors and cells do not directly determine age-related thymus changes in size throughout adult life.

We utilized intrathymic transplantation of TECs to evaluate the young and middle-aged thymic environments. TEC transplantation showed that middle-aged thymuses are highly permissive for TEC proliferation. Previous studies have suggested that the aged thymic environment, which accumulates significant numbers of adipocytes, may become hostile to TECs and impede thymocyte growth (21). Nevertheless, intrathymic transplantation indicated that middle-aged and young thymus environments were equally permissive for donor TEC proliferation.

Transplantation of fetal thymic cells into middle-aged thymuses drives thymus growth and increases naïve T cell production. The increases in naïve T cells detected in the spleens of recipient mice were modest, however, and did not correlate with engraftment levels. The lack of correlation between engraftment level and splenic naïve T cell frequency may have been due to the large natural variation in the frequencies of naïve T cells in the control middle-aged mice, together with the fact that the wild type mice used in this study already had “full” T cell niches, which may have decreased the efficiency with which new thymic emigrants survived in the periphery. Furthermore, it is possible that different classes of TECs engrafted in different mice, leading to additional variability in naïve T cell output.

We have not yet determined precisely which fetal TEC subset drives thymic growth in this model, however both mTECs and cTECs were abundant in the engrafted lobes. Fetal TEC progenitors that give rise to both mTECs and cTECs have been conclusively identified in the fetal thymus (56), and bipotent progenitors have recently been identified in the adult thymus (51). Our findings indicate that engraftable, colony forming TECs are abundant in the fetal and newborn thymus. Whether these postnatal TECs are bipotent progenitors, unipotent transient amplifying cells, or some mixture of the two is not known; however, the profound and rapid decrease in transplantable, colony forming TECs that occurs during the first 4 weeks of life suggests that these TECs are required or growth of the early thymus and that their loss spurs thymic involution.

Here we demonstrate that transplanted fetal TECs and progenitors can drive growth of the middle-aged thymus. Although further investigation will be required to identify the exact TEC subset that drives the thymic growth, this study provides proof-of-principle that intrathymic transplantation of TECs, either isolated from growing thymuses, or generated de novo from pluripotent stem cells (57), can be used for immune regeneration.

Supplementary Material

Refer to Web version on PubMed Central for supplementary material.

Acknowledgments

This study was funded by a Mary K. Iacocca Foundation Research Fellowship to MJK, and by a Harvard Stem Cell Institute Seed grant and a Program Project grant, and grants from the Peabody Foundation, The A&M Stewart Trust, The Fleischer Family Foundation, and the Pittsburgh Foundation to TS, and by grants from the Glenn Foundation for Medical Research and NIH to AJW (1R01 AG033053, 1DP2 OD004345, and 5U01 HL100402). This work was supported by an NIH Diabetes Research Center grant (P30DK036836).

We gratefully acknowledge Stephan Kissler, Aldo Rossini, and Martin Thelin for their input on the manuscript. The authors gratefully acknowledge the Joslin Diabetes Center Flow Cytometry Core, the Joslin Microscopy Core, and the Harvard Stem Cell Institute. We also thank Matt Levine for the use of the Keyence Microscope and software. The authors acknowledge the excellent support of the Joslin Animal Facility.

Abbreviations used in this article

TECs	thymic epithelial cells
cTECs	cortical thymic epithelial cells
mTECs	medullary thymic epithelial cells
RFP	red fluorescent protein
WT	wild type
KO	knockout
UEA	*Ulex Europaeus* Agglutinin I
EpCAM	epithelial cell adhesion molecule

References

1. Torroba M, Zapata AG. Aging of the vertebrate immune system. Microsc Res Tech. 2003; 62:477–481. [PubMed: 14635140]
2. Steinmann GG, Klaus B, Müller-Hermelink HK. The involution of the ageing human thymic epithelium is independent of puberty. A morphometric study. Scand J Immunol. 1985; 22:563–575. [PubMed: 4081647]
3. Sempowski GD, Gooding ME, Liao HX, Le PT, Haynes BF. T cell receptor excision circle assessment of thymopoiesis in aging mice. Mol Immunol. 2002; 38:841–848. [PubMed: 11922942]
4. Hale JS, Boursalian TE, Turk GL, Fink PJ. Thymic output in aged mice. Proc Natl Acad Sci USA. 2006; 103:8447–8452. [PubMed: 16717190]
5. Gui J, Mustachio LM, Su D-M, Craig RW. Thymus Size and Age-related Thymic Involution: Early Programming, Sexual Dimorphism, Progenitors and Stroma. Aging Dis. 2012; 3:280–290. [PubMed: 22724086]
6. Henderson J. On the relationship of the thymus to the sexual organs: I. The influence of castration on the thymus. J Physiol (Lond). 1904; 31:222–229. [PubMed: 16992746]
7. Olsen NJ, Watson MB, Henderson GS, Kovacs WJ. Androgen deprivation induces phenotypic and functional changes in the thymus of adult male mice. Endocrinology. 1991; 129:2471–2476. [PubMed: 1834454]
8. Greenstein BD, Fitzpatrick FTA, Adcock IM, Kendall MD, Wheeler MJ. Reappearance of the thymus in old rats after orchidectomy: inhibition of regeneration by testosterone. J Endocrinol. 1986; 110:417–422. [PubMed: 3760740]
9. Dracott BN, Smith CE. Hydrocortisone and the antibody response in mice. I. Correlations between serum cortisol levels and cell numbers in thymus, spleen, marrow and lymph nodes. Immunology. 1979; 38:429–435. [PubMed: 511224]

10. Jaffe HL. The influence of the suprarenal gland on the thymus: I. Regeneration of the thymus following double suprarenalectomy in the rat. J Exp Med. 1924; 40:325–342. [PubMed: 19868921]
11. Min D, Panoskaltsis-Mortari A, Kuro-O M, Holländer GA, Blazar BR, Weinberg KI. Sustained thymopoiesis and improvement in functional immunity induced by exogenous KGF administration in murine models of aging. Blood. 2007; 109:2529–2537. [PubMed: 17138819]
12. Chu Y-W, Schmitz S, Choudhury B, Telford W, Kapoor V, Garfield S, Howe D, Gress RE. Exogenous insulin-like growth factor 1 enhances thymopoiesis predominantly through thymic epithelial cell expansion. Blood. 2008; 112:2836–2846. [PubMed: 18658030]
13. Bolotin E, Smogorzewska M, Smith S, Widmer M, Weinberg K. Enhancement of thymopoiesis after bone marrow transplant by in vivo interleukin-7. Blood. 1996; 88:1887–1894. [PubMed: 8781449]
14. Dudakov JA, Hanash AM, Jenq RR, Young LF, Ghosh A, Singer NV, West ML, Smith OM, Holland AM, Tsai JJ, Boyd RL, van den Brink MRM. Interleukin-22 drives endogenous thymic regeneration in mice. Science. 2012; 336:91–95. [PubMed: 22383805]
15. Zediak VP, Maillard I, Bhandoola A. Multiple prethymic defects underlie age-related loss of T progenitor competence. Blood. 2007; 110:1161–1167. [PubMed: 17456721]
16. Min H, Montecino-Rodriguez E, Dorshkind K. Reduction in the developmental potential of intrathymic T cell progenitors with age. J Immunol. 2004; 173:245–250. [PubMed: 15210781]
17. Serwold T, Ehrlich LIR, Weissman IL. Reductive isolation from bone marrow and blood implicates common lymphoid progenitors as the major source of thymopoiesis. Blood. 2009; 113:807–815. [PubMed: 18927436]
18. Bhandoola A, Sambandam A. From stem cell to T cell: one route or many? Nat Rev Immunol. 2006; 6:117–126. [PubMed: 16491136]
19. Zhu X, Gui J, Dohkan J, Cheng L, Barnes PF, Su D-M. Lymphohematopoietic progenitors do not have a synchronized defect with age-related thymic involution. Aging Cell. 2007; 6:663–672. [PubMed: 17681038]
20. Mackall CL, Gress RE. Thymic aging and T-cell regeneration. Immunol Rev. 1997; 160:91–102. [PubMed: 9476668]
21. Dixit VD. Thymic fatness and approaches to enhance thymopoietic fitness in aging. Curr Opin Immunol. 2010; 22:521–528. [PubMed: 20650623]
22. Dixit VD, Yang H, Sun Y, Weeraratna AT, Youm Y-H, Smith RG, Taub DD. Ghrelin promotes thymopoiesis during aging. J Clin Invest. 2007; 117:2778–2790. [PubMed: 17823656]
23. Youm Y-H, Kanneganti T-D, Vandanmagsar B, Zhu X, Ravussin A, Adijiang A, Owen JS, Thomas MJ, Francis J, Parks JS, Dixit VD. The NLRP3 Inflammasome Promotes Age-Related Thymic Demise and Immunosenescence. Cell Reports. 2012; 1:56–68. [PubMed: 22832107]
24. Gray DHD, Seach N, Ueno T, Milton MK, Liston A, Lew AM, Goodnow CC, Boyd RL. Developmental kinetics, turnover, and stimulatory capacity of thymic epithelial cells. Blood. 2006; 108:3777–3785. [PubMed: 16896157]
25. Chen L, Xiao S, Manley NR. Foxn1 is required to maintain the postnatal thymic microenvironment in a dosage-sensitive manner. Blood. 2009; 113:567–574. [PubMed: 18978204]
26. Markowitz JS, Auchincloss H, Grusby MJ, Glimcher LH. Class II-positive hematopoietic cells cannot mediate positive selection of CD4+ T lymphocytes in class II-deficient mice. Proc Natl Acad Sci USA. 1993; 90:2779–2783. [PubMed: 8464889]
27. Moore NC, Anderson G, Smith CA, Owen JJ, Jenkinson EJ. Analysis of cytokine gene expression in subpopulations of freshly isolated thymocytes and thymic stromal cells using semiquantitative polymerase chain reaction. Eur J Immunol. 1993; 23:922–927. [PubMed: 8458378]
28. Koch U, Fiorini E, Benedito R, Besseyrias V, Schuster-Gossler K, Pierres M, Manley NR, Duarte A, MacDonald HR, Radtke F. Delta-like 4 is the essential, nonredundant ligand for Notch1 during thymic T cell lineage commitment. J Exp Med. 2008; 205:2515–2523. [PubMed: 18824585]
29. Zamisch M, Moore-Scott B, Su D-M, Lucas PJ, Manley N, Richie ER. Ontogeny and regulation of IL-7-expressing thymic epithelial cells. J Immunol. 2005; 174:60–67. [PubMed: 15611228]
30. Takahama Y. Journey through the thymus: stromal guides for T-cell development and selection. Nat Rev Immunol. 2006; 6:127–135. [PubMed: 16491137]

31. Garfin PM, Min D, Bryson JL, Serwold T, Edris B, Blackburn CC, Richie ER, Weinberg KI, Manley NR, Sage J, Viatour P. Inactivation of the RB family prevents thymus involution and promotes thymic function by direct control of Foxn1 expression. J Exp Med. 2013; 210:1087–1097. [PubMed: 23669396]
32. Klug DB, Crouch E, Carter C, Coghlan L, Conti CJ, Richie ER. Transgenic expression of cyclin D1 in thymic epithelial precursors promotes epithelial and T cell development. J Immunol. 2000; 164:1881–1888. [PubMed: 10657637]
33. Nehls M, Pfeifer D, Schorpp M, Hedrich H, Boehm T. New member of the winged-helix protein family disrupted in mouse and rat nude mutations. Nature. 1994; 372:103–107. [PubMed: 7969402]
34. Jenkinson WE, Bacon A, White AJ, Anderson G, Jenkinson EJ. An epithelial progenitor pool regulates thymus growth. J Immunol. 2008; 181:6101–6108. [PubMed: 18941199]
35. Bredenkamp N, Nowell CS, Blackburn CC. Regeneration of the aged thymus by a single transcription factor. Development. 2014; 141:1627–1637. [PubMed: 24715454]
36. Sun L, Guo J, Brown R, Amagai T, Zhao Y, Su D-M. Declining expression of a single epithelial cell-autonomous gene accelerates age-related thymic involution. Aging Cell. 2010; 9:347–357. [PubMed: 20156205]
37. Wright DE, Cheshier SH, Wagers AJ, Randall TD, Christensen JL, Weissman IL. Cyclophosphamide/granulocyte colony-stimulating factor causes selective mobilization of bone marrow hematopoietic stem cells into the blood after M phase of the cell cycle. Blood. 2001; 97:2278–2285. [PubMed: 11290588]
38. Ueno H, Weissman IL. Clonal Analysis of Mouse Development Reveals a Polyclonal Origin for Yolk Sac Blood Islands. Dev Cell. 2006; 11:519–533. [PubMed: 17011491]
39. Wright DE, Wagers AJ, Gulati AP, Johnson FL, Weissman IL. Physiological migration of hematopoietic stem and progenitor cells. Science. 2001; 294:1933–1936. [PubMed: 11729320]
40. Loffredo FS, Steinhauser ML, Jay SM, Gannon J, Pancoast JR, Yalamanchi P, Sinha M, Dall'Osso C, Khong D, Shadrach JL, Miller CM, Singer BS, Stewart A, Psychogios N, Gerszten RE, Hartigan AJ, Kim M-J, Serwold T, Wagers AJ, Lee RT. Growth Differentiation Factor 11 Is a Circulating Factor that Reverses Age-Related Cardiac Hypertrophy. Cell. 2013; 153:828–839. [PubMed: 23663781]
41. Jerabek L, Weissman IL. Intrathymic injection for analysis of T-cell progenitor activity. Methods Mol Med. 2002; 63:161–165. [PubMed: 21437807]
42. Ruckh JM, Zhao J-W, Shadrach JL, van Wijngaarden P, Rao TN, Wagers AJ, Franklin RJM. Rejuvenation of regeneration in the aging central nervous system. Cell Stem Cell. 2012; 10:96–103. [PubMed: 22226359]
43. Sinha M, Jang YC, Oh J, Khong D, Wu EY, Manohar R, Miller C, Regalado SG, Loffredo FS, Pancoast JR, Hirshman MF, Lebowitz J, Shadrach JL, Cerletti M, Kim M-J, Serwold T, Goodyear LJ, Rosner B, Lee RT, Wagers AJ. Restoring systemic GDF11 levels reverses age-related dysfunction in mouse skeletal muscle. Science. 2014; 344:649–652. [PubMed: 24797481]
44. Conboy IM, Conboy MJ, Wagers AJ, Girma ER, Weissman IL, Rando TA. Rejuvenation of aged progenitor cells by exposure to a young systemic environment. Nature. 2005; 433:760–764. [PubMed: 15716955]
45. Brack AS, Conboy MJ, Roy S, Lee M, Kuo CJ, Keller C, Rando TA. Increased Wnt signaling during aging alters muscle stem cell fate and increases fibrosis. Science. 2007; 317:807–810. [PubMed: 17690295]
46. Villeda SA, Luo J, Mosher KI, Zou B, Britschgi M, Bieri G, Stan TM, Fainberg N, Ding Z, Eggel A, Lucin KM, Czirr E, Park J-S, Couillard-Després S, Aigner L, Li G, Peskind ER, Kaye JA, Quinn JF, Galasko DR, Xie XS, Rando TA, Wyss-Coray T. The ageing systemic milieu negatively regulates neurogenesis and cognitive function. Nature. 2011; 477:90–94. [PubMed: 21886162]
47. Donskoy E, Goldschneider I. Thymocytopoiesis is maintained by blood-borne precursors throughout postnatal life. A study in parabiotic mice. J Immunol. 1992; 148:1604–1612. [PubMed: 1347301]
48. Inlay MA, Bhattacharya D, Sahoo D, Serwold T, Seita J, Karsunky H, Plevritis SK, Dill DL, Weissman IL. Ly6d marks the earliest stage of B-cell specification and identifies the branchpoint

between B-cell and T-cell development. Genes & Development. 2009; 23:2376–2381. [PubMed: 19833765]

49. Cosgrove D, Gray D, Dierich A, Kaufman J, Lemeur M, Benoist C, Mathis D. Mice lacking MHC class II molecules. Cell. 1991; 66:1051–1066. [PubMed: 1909605]
50. Watanabe K, Ueno M, Kamiya D, Nishiyama A, Matsumura M, Wataya T, Takahashi JB, Nishikawa S, Nishikawa S-I, Muguruma K, Sasai Y. A ROCK inhibitor permits survival of dissociated human embryonic stem cells. Nat Biotechnol. 2007; 25:681–686. [PubMed: 17529971]
51. Wong K, Lister NL, Barsanti M, Lim JMC, Hammett MV, Khong DM, Siatskas C, Gray DHD, Boyd RL, Chidgey AP. Multilineage potential and self-renewal define an epithelial progenitor cell population in the adult thymus. Cell Reports. 2014; 8:1198–1209. [PubMed: 25131206]
52. Linton PJ, Dorshkind K. Age-related changes in lymphocyte development and function. Nat Immunol. 2004; 5:133–139. [PubMed: 14749784]
53. Sudo K, Ema H, Morita Y, Nakauchi H. Age-associated characteristics of murine hematopoietic stem cells. J Exp Med. 2000; 192:1273–1280. [PubMed: 11067876]
54. Rossi DJ, Bryder D, Zahn JM, Ahlenius H, Sonu R, Wagers AJ, Weissman IL. Cell intrinsic alterations underlie hematopoietic stem cell aging. Proc Natl Acad Sci USA. 2005; 102:9194–9199. [PubMed: 15967997]
55. Pishel I, Shytikov D, Orlova T, Peregudov A, Artyuhov I, Butenko G. Accelerated aging versus rejuvenation of the immune system in heterochronic parabiosis. Rejuvenation Res. 2012; 15:239–248. [PubMed: 22533440]
56. Rossi SW, Jenkinson WE, Anderson G, Jenkinson EJ. Clonal analysis reveals a common progenitor for thymic cortical and medullary epithelium. Nature. 2006; 441:988. [PubMed: 16791197]
57. Inami Y, Yoshikai T, Ito S, Nishio N, Suzuki H, Sakurai H, Isobe KI. Differentiation of induced pluripotent stem cells to thymic epithelial cells by phenotype. Immunol Cell Biol. 2011; 89:314–321. [PubMed: 20680027]

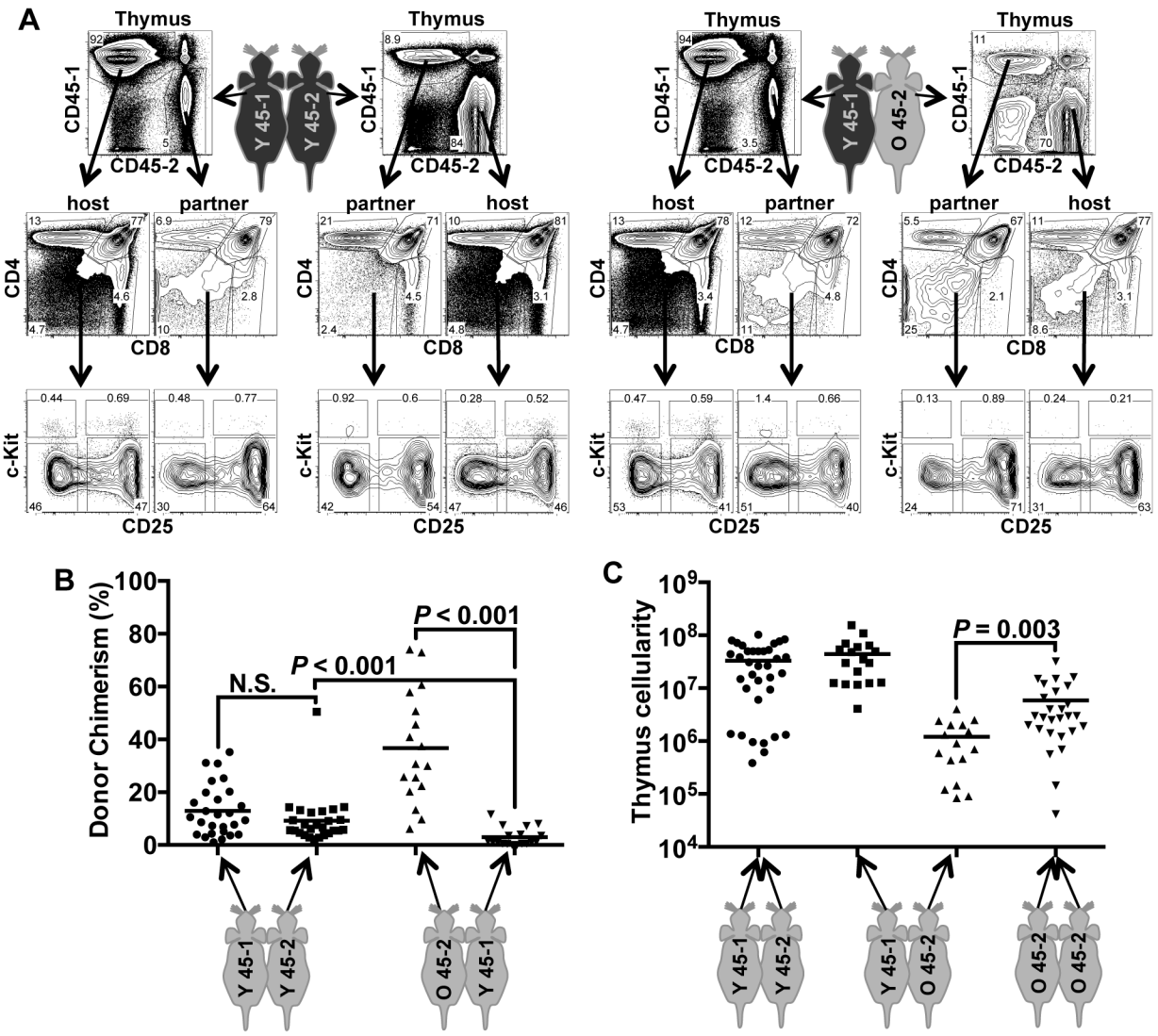

Figure 1.

Heterochronic parabiosis leads to colonization, but not regeneration, of aged thymuses. Pairs of isochronic young (2 months old), isochronic old (21–23 months old), or heterochronic young and aged mice (2 months and 21–23 months old) were parabiosed. After 30 days, thymuses were removed, dispersed and analyzed by cell counting and by flow cytometry. (A) Young:young (Y 45-1, Y 45-2) and young:aged (Y45-1, O45-2) pairs expressed distinct CD45 alleles and were analyzed for thymic chimerism. Each pair contributed thymocytes to one another, and these were analyzed for developmental progression using markers of thymocyte subsets, CD4, CD8, c-Kit, and CD25. “Thymus” plots were pre-gated on live cells. Middle plots show CD4 vs. CD8 stains of live thymocytes. Lower plots show cells gated on $CD3^{-}$, $CD4^{-}$, $CD8^{-}$, non-B, and non-myeloid lineages, and show c-Kit vs. CD25 expression. $c\text{-}Kit^{+}CD25^{-}$ cells represent the earliest thymocyte progenitors (ETP or DN1), followed by $c\text{-}Kit^{+}CD25^{+}$ (DN2), $c\text{-}Kit^{-}CD25^{+}$ (DN3), and $c\text{-}Kit^{-}CD25^{-}$ (DN4) populations. (B) Donor chimerism within each isochronic and heterochronic pair was determined by staining for CD45-1 and CD45-2, as in A. Each point represents the

chimerism of one parabiotic mouse. (C) Total thymus cellularity of each parabiotic mouse was determined by cell counting. *P* values were determined using the unpaired Student's *t* test. Mean values are shown as lines on each plot.

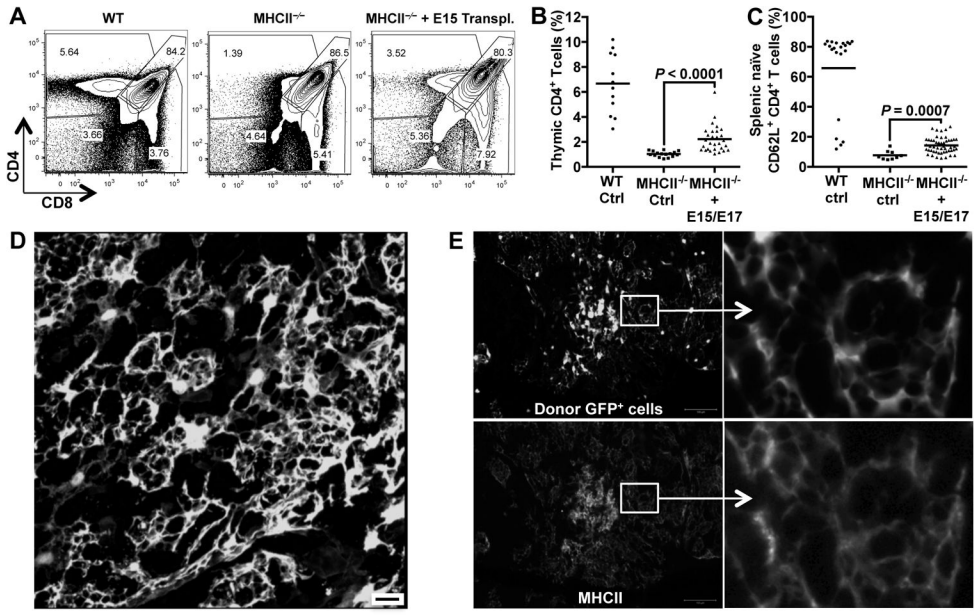

Figure 2.

Intrathymically injected TECs engraft and function *in vivo.* Thymic cells were prepared from E15 or E17 GFP-transgenic fetuses and injected into the thymuses of MHCII$^{-/-}$ mice (1–3 months old). After one month, thymocytes and splenocytes of transplanted mice were analyzed. Wild type (WT) and non-transplanted MHCII$^{-/-}$ mice were analyzed as controls. (A) Thymocytes were stained with antibodies to CD4 and CD8 and analyzed by flow cytometry. Plots are pre-gated on live, GFP^{-} host-derived cells. Plots are derived from representative mice analyzed in Figure 2B. (B) The plot shows the percentages of thymic CD4^{+} T cells from control mice or mice intrathymically injected with E15/E17 dispersed thymic cells. Each point represents the percentage of CD4^{+} T cells from one animal. Mean values are shown as a bar. (C) Splenocytes from the control and transplanted animals were stained with CD4, CD8, TCRβ, CD44, and CD62L. Cells were gated on CD4^{+}TCRβ^{+} T cells and analyzed for CD62L and CD44 expression. Each point represents splenocytes from one animal. Mean values are shown as a bar. (D) Total thymic cells from P1 GFP-transgenic mice were intrathymically injected into one-month old WT mice. After one month, recipient thymuses were fixed in PFA, sectioned and examined for engraftment of GFP^{+} cells by confocal microscopy. Scale bar represents 20 μm. The image is representative among sections from five mice in this experiment. (E) Thymic cells derived from P3 and P5 GFP-transgenic mice were column purified to select EpCAM^{+} TECs and then injected into one-month old MHCII$^{-/-}$ male mice. After one month, thymuses were removed and PFA fixed and thymic sections were analyzed for donor cell engraftment and MHCII expression. GFP^{+} donor TECs are shown in the top panels. MHCII expression was detected by antibody staining (bottom panels). Both GFP and MHCII signals are shown in gray scale. Scale bar represents 100 μm. Enlarged areas are shown at right. The experiment was repeated more than 10 times, and a representative section is shown here. *P* values were determined using the unpaired Student's *t*-test.

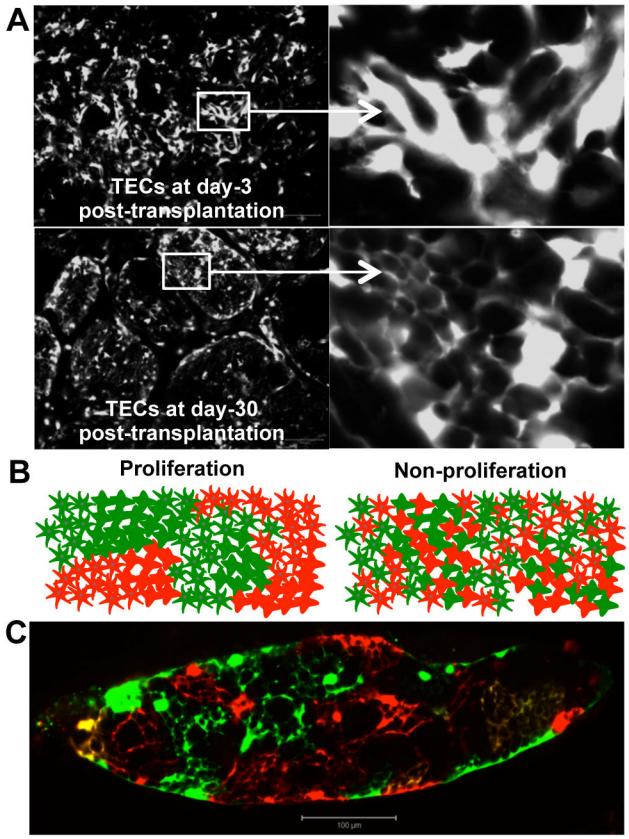

Figure 3.

Intrathymically transplanted TECs proliferate *in vivo.* (A) Thymic cells were isolated from P1 GFP transgenic mice and injected into 3-month old MHCII$^{-/-}$ mice. After 3 days (top panels) or 30 days (bottom panels), recipient thymuses were fixed in PFA, sectioned and analyzed for GFP-fluorescence (gray scale, scale bar represents 100 μm). Boxed areas are enlarged and shown on right. Thymuses from 5 recipient mice were analyzed at each time point, and images from one engrafted mouse at each time point are shown. (B) Drawings show predicted outcomes of injections of mixed GFP^{+} and RFP^{+} TECs that distinguish between TECs that both form networks and proliferate (left drawing) and TECs that form networks without proliferating (right drawing).(C) Purified TECs from P5 GFP-transgenic and RFP-transgenic mice were co-injected into 6-month old MHCII$^{-/-}$ recipients. After one month, thymuses were removed and PFA fixed, and tissue sections were examined by fluorescence microscopy (scale bar represents 100 μm, n = 5 intrathymically transplanted mice).

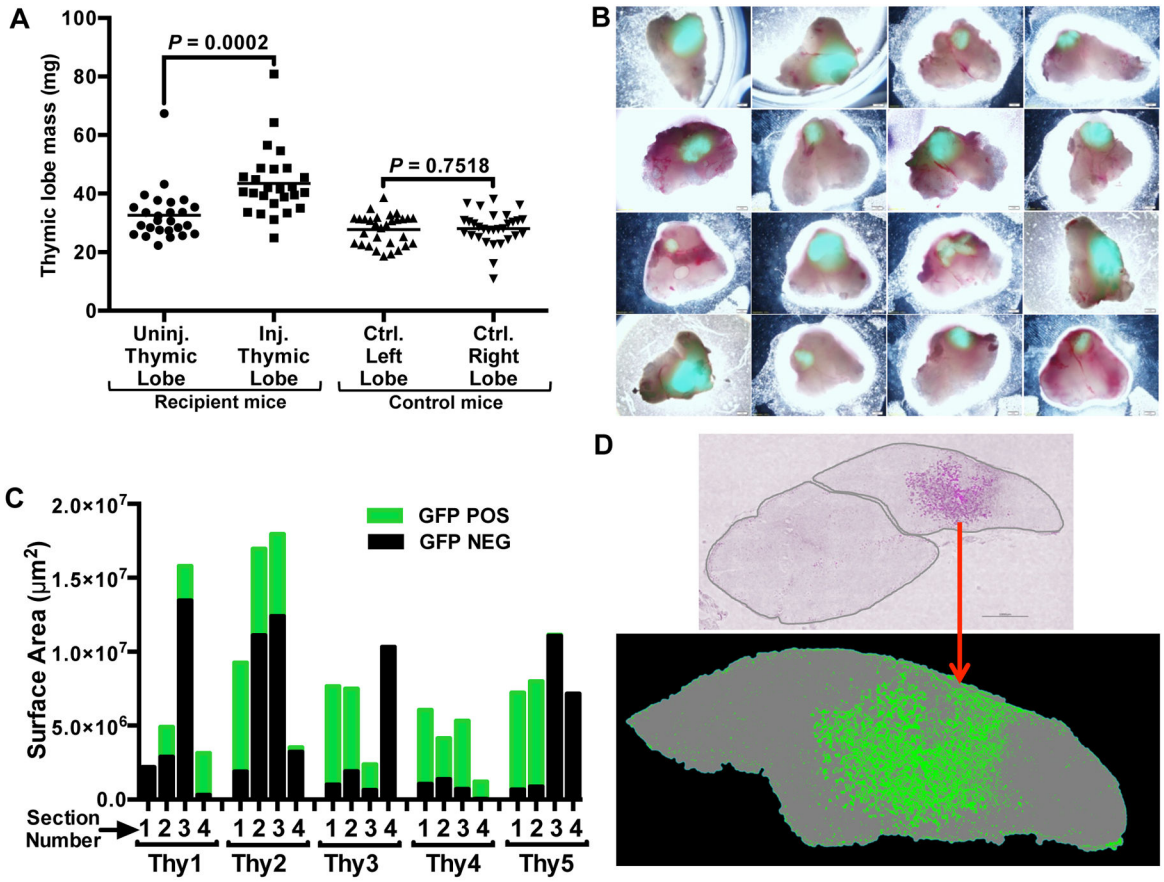

Figure 4.

Transplantation of fetal thymic cells drives growth of middle-aged thymuses. Single cell suspensions of thymic cells were prepared from GFP-transgenic E14.5 or E15.5 fetal thymuses and injected into one thymic lobe of each middle-aged (9–12 months old) WT female mouse. After 45 days, thymuses and spleens of recipient and control mice were removed and analyzed. (A) Injected (Inj.) and uninjected (Uninj.) thymic lobes, and lobes from control (Ctrl.) mice were separated and individually weighed. Each point represents the mass of an individual thymic lobe. Mean values for each group are shown as bars. (B) Representative recipient thymuses were imaged with an inverted fluorescence microscope 45 days after injection of dispersed GFP^+ thymic cells. (C) Five representative thymuses were completely sectioned into 100–200 sections, and the area of GFP engraftment was determined in 4 sections, each 25 sections apart, within each thymus. (D) A representative thymic section from an intrathymically injected recipient is shown. The top image shows both thymic lobes; donor GFP^+ cells are pseudo-colored magenta within the lobe on the right. The bottom image shows a binary image with the donor cells shown in green and the thymic lobe in gray. *P* values were determined using the paired Student's *t*-test. The number of cells injected into each mouse ranged from 1×10^5–1×10^6.

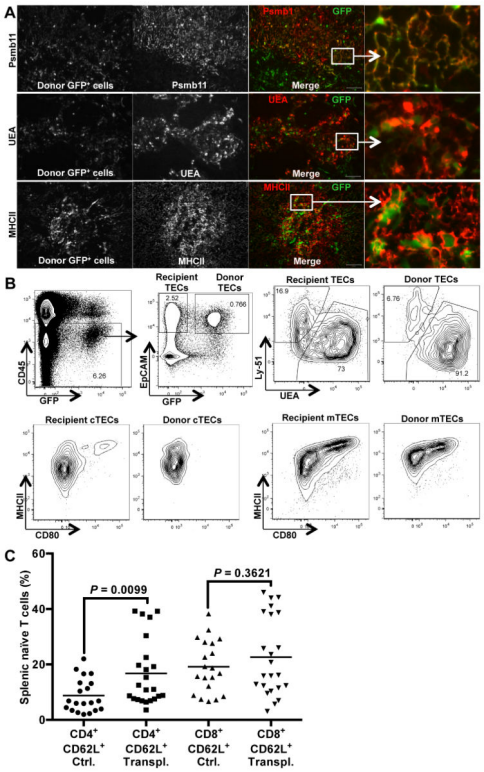

Figure 5.

Thymic epithelial cells engraft and maintain functional phenotypes upon intrathymic transplantation. (A) Sections from recipient thymuses from Figure 4 were fixed in PFA, and analyzed for GFP^+ engrafted cells (first column). Sections were analyzed for co-expression of GFP and Psmb11 (top row), UEA (middle row), and MHCII (bottom row), $Psmb11^+$, UEA^+, and $MHCII^+$ cells are shown in gray scale (second column). In merged images (third and fourth columns), GFP^+ cells are shown in green, and $Psmb11^+$, UEA^+, or $MHCII^+$ cells in red. Boxed areas are zoomed in and shown in the fourth column. Scale bar represents 100 μm. The images are representative of 5 recipient thymuses. (B) Thymuses from transplanted mice shown in Figure 4A and 4B were enzymatically dissociated into single cells. Isolated cells were stained for CD45, EpCAM, MHCII, Ly-51, UEA and CD80 and analyzed by flow cytometry. Plots show one well-engrafted thymus, from more than 10 similar experiments. The gating strategy to identify donor TECs is shown ($CD45^-$, GFP^+, and $EpCAM^+$). Donor-derived TECs and endogenous recipient TECs were further analyzed for the expression of Ly-51 (cTECs) and UEA (mTECs). (C) Splenocytes from transplanted (Transpl.) and control (Ctrl.) mice shown in Figure 4A and 4B were prepared into single cells and stained for CD4, CD8, CD44 and CD62L to distinguish naïve and memory T cells. The percentages of naïve $CD62L^+CD4^+$ cells and naïve $CD62L^+CD8^+$ cells within the total $CD4^+$ and $CD8^+$ populations, respectively, are shown in the graph. Mean values for each group are shown as bars. *P* values were determined using the unpaired Student's *t*-test

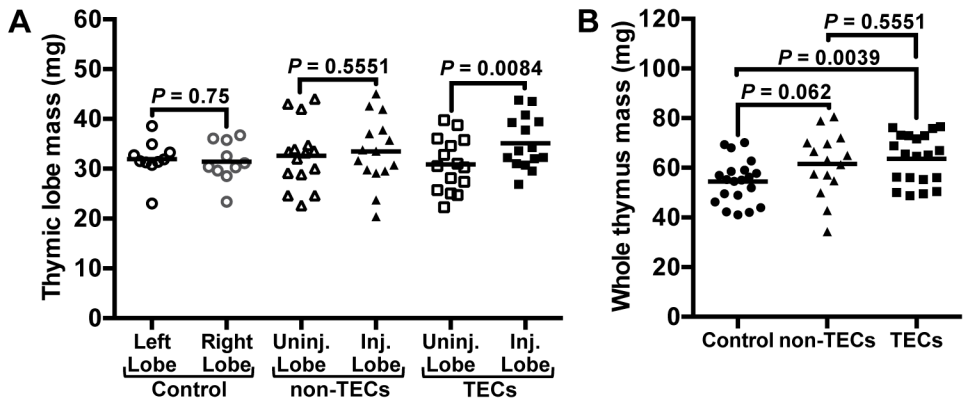

Figure 6.

Purified thymic epithelial cells drive thymic growth. TECs ($CD45^{-}EpCAM^{+}$) and non-TECs ($CD45^{+}EpCAM^{-}$, including all live cells that did not fall into the TEC gate) were sorted from GFP^{+} fetal thymuses, and were injected into one thymic lobe of each middle-aged recipient mouse. Each mouse received 60,000–71,000 TECs or 360,000–400,000 non-TECs. After 45 days, thymuses were recovered and weighed. (A) Individual injected (Inj.) and uninjected (Uninj.) lobes were weighed from experimental mice. Left and Right lobes were compared in control mice. (B) Whole thymuses from control mice and mice that were intrathymically injected with either TECs or non-TECs were weighed. *P* values were determined using the paired (A) and unpaired (B) Student's *t*-tests

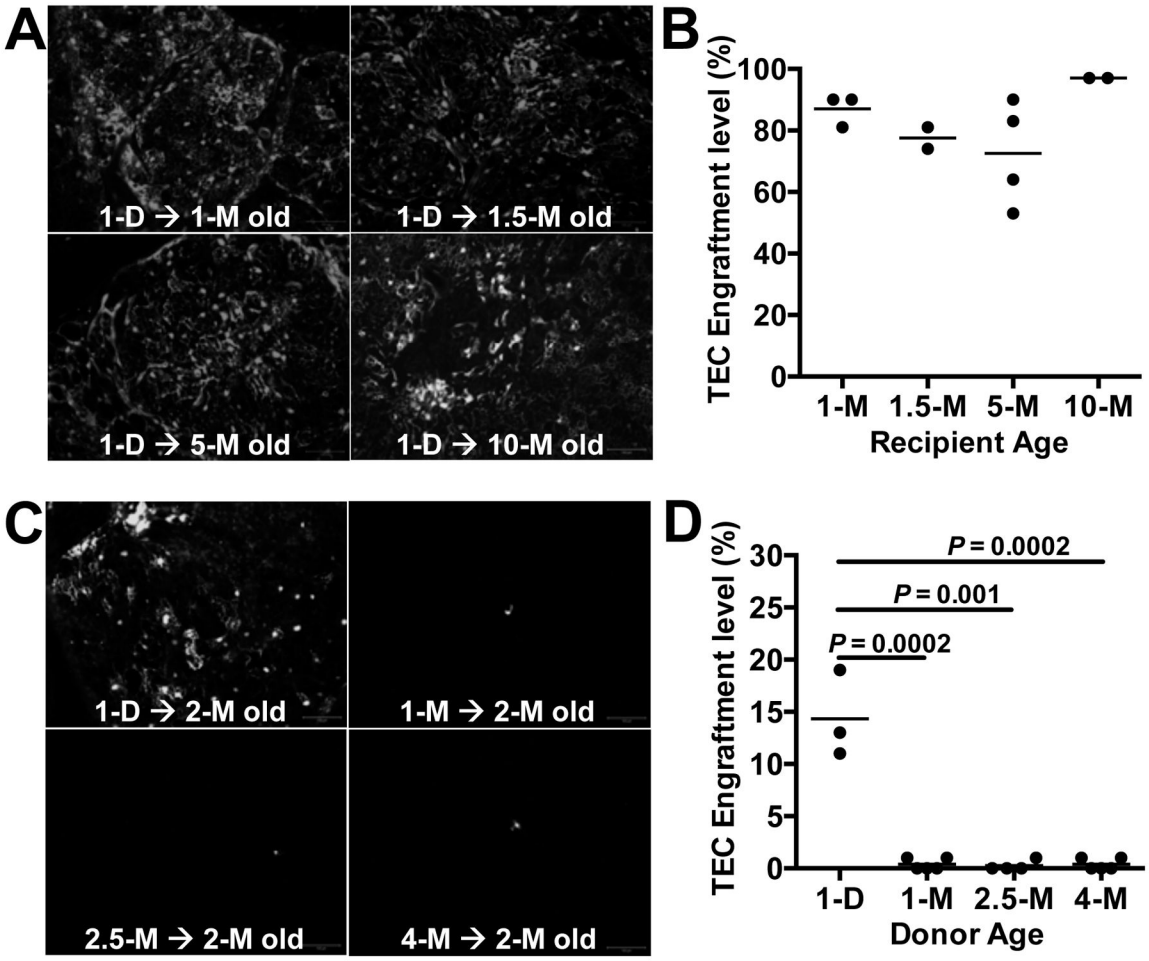

Figure 7.

The thymus retains its ability to be engrafted by TECs regardless of recipient age, but TECs lose their engraftment potential rapidly with donor age. (A) Thymic cells were prepared from P1 GFP-transgenic or RFP-transgenic mice, and equal numbers of EpCAM-enriched TECs were intrathymically injected into 1–10-month old WT mice. After one month, thymuses were PFA-fixed, and completely sectioned (100–200 sections per thymus) and were examined by fluorescence microscopy. Representative sections are shown, and donor cells are shown in gray-scale. (B) Each section was analyzed for the presence of donor cells, and the percentage of sections that contained donor cells within each recipient thymus was determined. Each point on the plot represents the percentage of donor-cell-containing sections within one recipient thymus. Mean values are shown for each experimental group. (C) Equal numbers of EpCAM enriched TECs from GFP-transgenic mice of the indicated ages were intrathymically injected into 2-month old WT mice. After one month, thymuses were recovered and GFP^+ cells were detected by fluorescence microscopy. Donor cells are shown in gray scale. (D) Recipient thymuses were analyzed as in (B). Scale bar represents 100 μm. Day and month are shown as D and M, respectively. *P* values were determined using the unpaired Student's *t*-test.

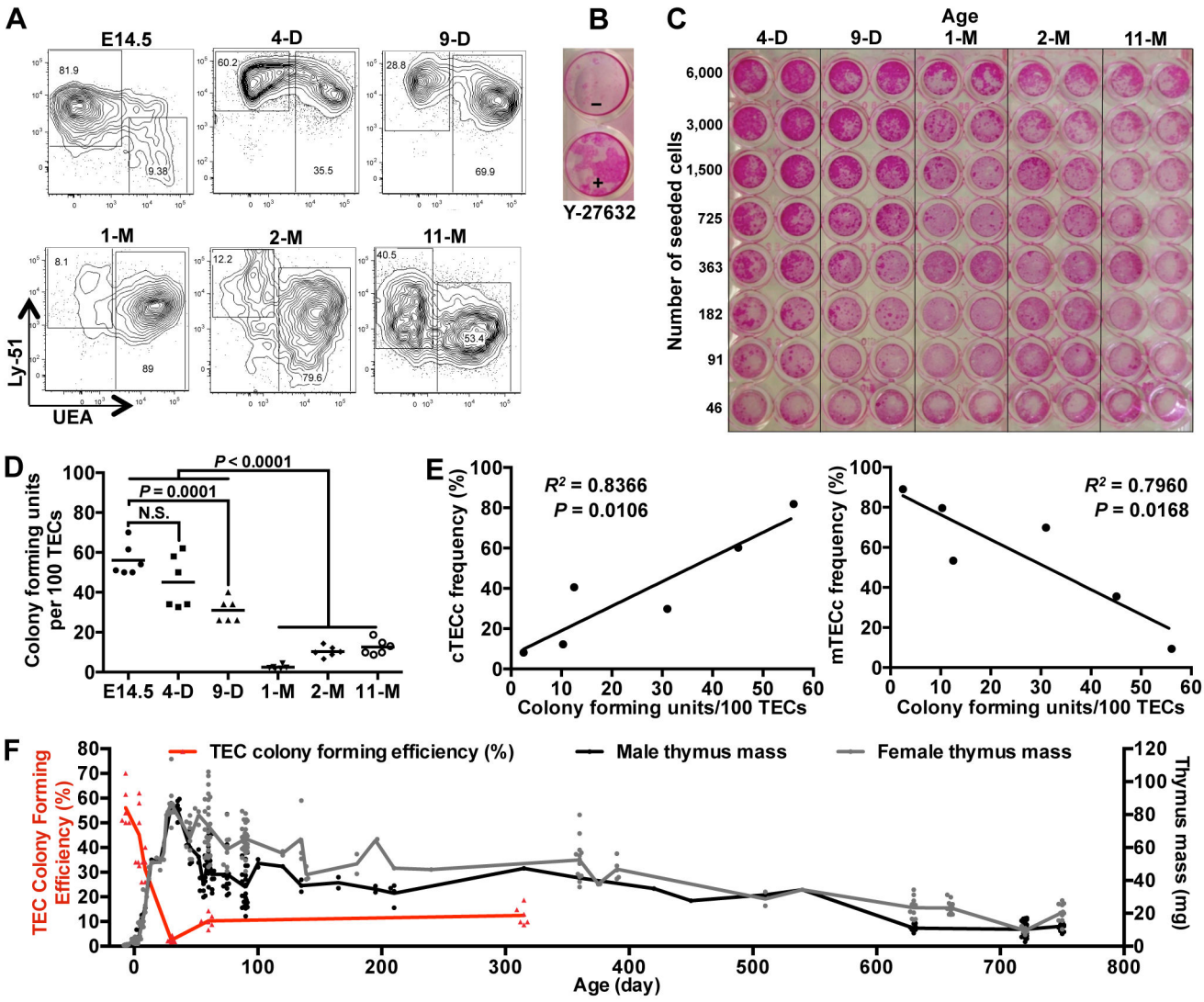

Figure 8.

The *in vitro* proliferative capacity of TECs declines rapidly with age. (A) Thymuses of E14.5, 4-day (4-D), 9-day (9-D), 1-month (1-M), 2-month (2-M), and 11-month (11-M) old GFP-transgenic mice were proteolytically digested, stained for TEC markers and analyzed by flow cytometry. Each plot shows TECs that were pre-gated on live, $CD45^{-}EpCAM^{+}$ cells. (B) Sorted $CD45^{-}EpCAM^{+}Ly\text{-}51^{+}$ TECs were seeded onto irradiated MEFs (800 TECs/well) in the presence or absence of ROCK inhibitor, Y-27632. After two weeks, wells were fixed and stained with Rhodamine B to visualize colonies. TEC colonies appear as dark red spots within the wells. The experiment is representative of more than 10 similar experiments. (C) Live, $CD45^{-}$, $EpCAM^{+}$ cells from (A) were sorted and plated in a 96-well plate at the indicated cell numbers per well in the presence of Y-27632. At 8-days post-seeding, colonies were visualized as in (B). Image represents one of two separate experiments. (D) GFP^{+} TEC colonies from each well were manually counted under an inverted fluorescence microscope on day 5 of the culture (prior to fixing in PFA, as shown in (C)). Each point on the graph represents the number of TEC colonies per 100 TECs

plated, determined from 6 wells that contained large numbers of distinct, separate colonies. Mean colony counts are shown as bars. (E) The percentages of TEC colony forming units as shown in (D) are plotted against cTEC and mTEC frequencies as shown in (A). (F) Thymus masses of mice of the indicated ages were measured and plotted together with the data from TEC colony forming unit efficiency (D). *P* values were determined using the unpaired Student's *t*-test (D) or *F*-test (E).